Application of integrated geophysical modeling for determination of the continental lithospheric thermal structure in the eastern Carpathians

Jana Dérerová,[1] Hermann Zeyen,[2] Miroslav Bielik,[3] and Karmah Salman[2]

Received 6 July 2005; revised 28 February 2006; accepted 13 March 2006; published 24 May 2006.

[1] We applied integrated lithospheric modeling combining the interpretation of surface heat flow, geoid, gravity, and topography data for the determination of the lithospheric thermal structure along four transects crossing the eastern Carpathians from the European Platform to the Pannonian Basin and propose a new map of lithospheric thicknesses. Important differences in lithospheric thickness across the chain as well as along strike of the Carpathian arc exist. Lithosphere thickness varies from 240 km in the foreland to 75–110 km, under the Pannonian Basin and it increases from the western to the eastern Carpathians. Under the western segment of the western Carpathians (in the transition zone to the eastern Alps), no thickening is observed, which may be explained by a mainly strike-slip movement between the European and Carpatho-Pannonian plates. Thickened lithosphere is found NE of thickened crust under the Carpathians. This observation is in agreement with slab roll-back and possible subsequent break-off. **Citation:** Dérerová, J., H. Zeyen, M. Bielik, and K. Salman (2006), Application of integrated geophysical modeling for determination of the continental lithospheric thermal structure in the eastern Carpathians, *Tectonics*, *25*, TC3009, doi:10.1029/2005TC001883.

1. Introduction

[2] The Carpathian-Pannonian region offers an outstanding opportunity to study the interaction of asthenospheric and lithospheric processes and their mutual dependencies during the orogeny, volcanic arc and related fore-arc and back-arc basin development. The Carpathian chain extends over a distance of nearly 1500 km and forms an arc of over 250° (Figure 1). The arc is unique in providing an onshore snapshot of a still active, soft collision between the Carpatho-Pannonian microplates and the European Platform [*Tomek and PANCARDI Colleagues*, 1996].

[3] A large diversity of geophysical methods has been used to investigate the lithosphere of the Carpathian-Pannonian region, such as deep seismic sounding (refraction and reflection seismics), seismology, seismic tomography, gravimetry, magnetometry, magnetotellurics and geothermics. However, the data of different geophysical fields used for the determination of the structure and geodynamics of the lithosphere have been interpreted separately. The analysis of the different models of the lithospheric thickness in central Europe defined by interpretation of teleseismic P wave delay times [*Babuška et al.*, 1987, 1988], magnetotelluric measurements [*Ádám*, 1976, 1996; *Praus et al.*, 1990] and geothermal modeling [*Čermák*, 1982, 1994; *Majcin*, 1994; *Majcin et al.*, 1998] has shown differences and problems related to those single-method interpretations [*Zeyen et al.*, 2002]. This led us to the application of integrated lithospheric modeling.

[4] In this paper, we present two-dimensional numerical models of the thermal and density structure of the continental lithosphere in the eastern Carpathians based on an integrated geophysical method, which combines interpretation of heat flow, absolute topographic elevation, gravity and geoid data. The main aim of this study is to model the lithosphere thickness and the actual temperature distribution along four transects crossing the eastern Carpathians and its surrounding tectonic units–the European Platform and the Pannonian Basin. These calculations represent a continuation in our systematic study of the thermal structure of the lithosphere in the Carpathian orogen. Lithospheric cross sections through the western Carpathians have already been published by *Zeyen and Bielik* [2000] and *Zeyen et al.* [2002]. On the basis of all our calculations, we propose a new map of the lithosphere thickness in the Carpathian-Pannonian region modified with respect to those presented by *Babuška et al.* [1988], *Horváth* [1993], *Lillie et al.* [1994], *Šefara et al.* [1996] and *Lenkey* [1999]. This map may serve as base for geodynamical reconstructions of this region and for a better understanding of the lithospheric processes governing its geodynamical evolution.

2. Tertiary Evolution of the Carpathian Chain and Pannonian Basin

[5] The Carpathian-Pannonian domain is located in an embayment of the European Platform. The northwestern tip of the embayment is bordered by the Bohemian Massif and

[1]Geophysical Institute of the Slovak Academy of Sciences, Bratislava, Slovak Republic.
[2]Département des Sciences de la Terre, Université de Paris-Sud, UMR 8146, Orsay, France.
[3]Faculty of Natural Sciences, Department of Applied and Environmental Geophysics, Comenius University, Bratislava, Slovak Republic.

0278-7407/06/2005TC001883$12.00

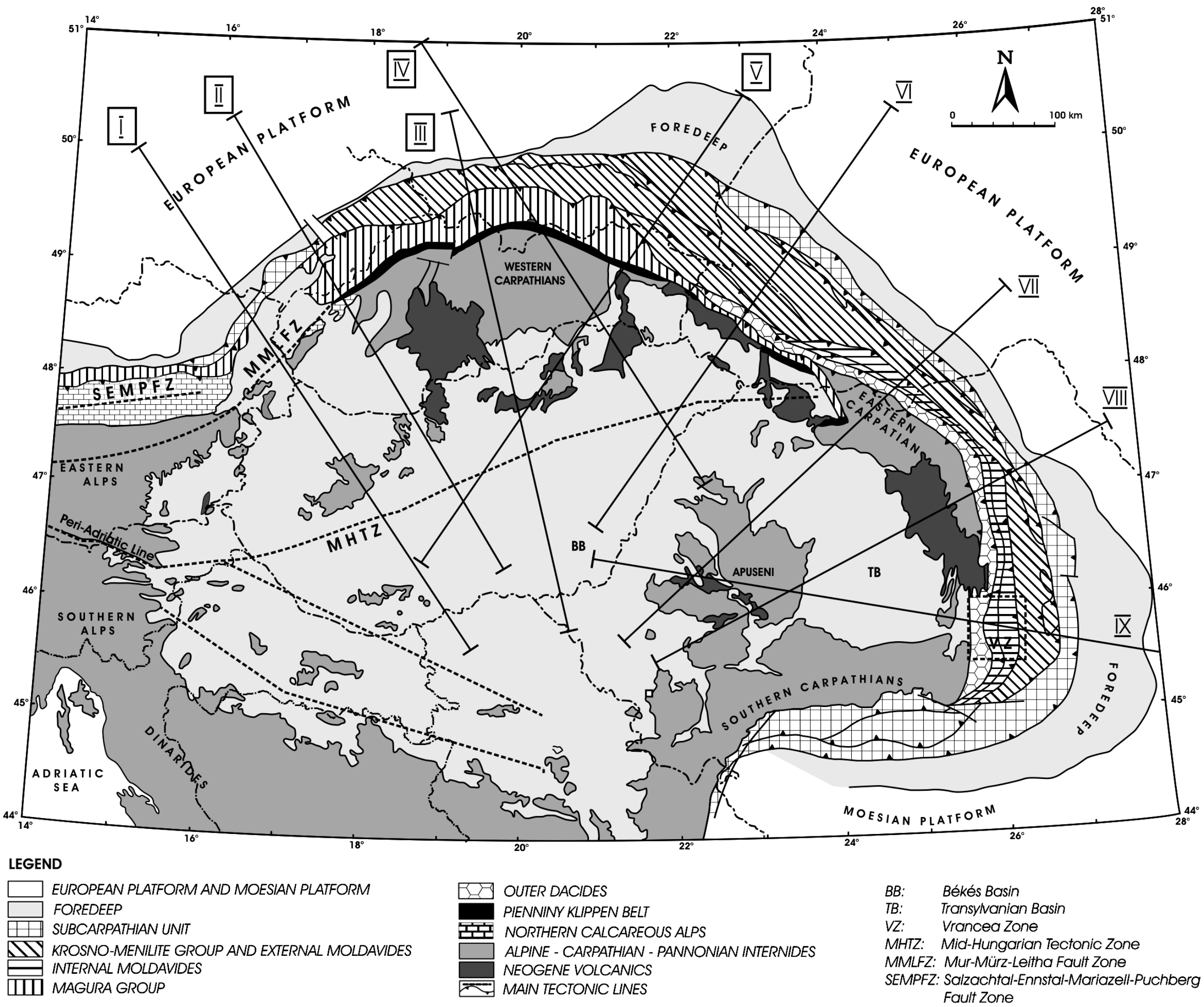

Figure 1. Schematic tectonic map of the Carpathian-Pannonian region (modified after *Kováč* [2000]) with location of the presented transects VI, VII, VIII, and IX. Transects I to V are transects published by *Zeyen et al.* [2002].

the southeastern tip by the Moesian Platform. The integrating element of the Carpathian system is the outer western Carpathian Flysch belt unit deposit on oceanic crust for the pre-Oligocene evolution [*Tari et al.*, 1993] and/or thinned continental crust [*Winkler and Slaczka*, 1992; *Sperner et al.*, 2002]. In front of the western Carpathian Flysch zone, the foredeep basin is extending onto the flexurally bent platform slope.

[6] After *Sperner et al.* [2001], Tertiary evolution of the Alpine-Carpathian orogen was characterized by the influence of SW to W dipping subduction. Originally, this subduction was active along the whole Alpine-Carpathian arc. However, after Eocene continental collision in the Alps, subduction continued in the Carpathians only, where an embayment in the European continental passive margin provided space for further subduction.

[7] Tertiary evolution of the Carpathians and Pannonian back-arc basin area was interpreted by *Konečný et al.* [2002] in terms of the coupled system of (1) Alpine subduction and compressive orogenic belt development, (2) lateral extrusion of the Alcapa (Alps-Carpathian-Pannonian) lithosphere along transform faults during the Alpine collision, (3) Carpathian gravity-driven subduction of oceanic or strongly thinned continental lithosphere underlying former flysch basins and (4) back-arc extension associated with the diapiric upwelling of asthenospheric mantle.

[8] Though the subduction and related asthenospheric mantle upwelling were always contemporaneous in any given segment of the Carpatho-Pannonian system they did not take place at the same time in the whole area. A wealth of observations indicates rather a progression from the west to the east and southeast [*Royden and Horváth*, 1988; *Rumpler and Horváth*, 1988; *Ratschbacher et al.*, 1991a, 1991b; *Csontos et al.*, 1992; *Horváth*, 1993; *Tomek and Hall*, 1993; *Linzer*, 1996; *Kováč et al.*, 1998; *Kováč*, 2000; *Konečný et al.*, 2002].

Table 1. Densities and Thermal Properties of the Different Bodies Used in the Transects[a]

No.	Unit	HP	TC	ρ_0
1	Neogene sediments	3.0–3.5	2.0–2.5	2400–2550
2	flysch, foreland basin, sedimentary cover of European Platform	1.0–2.5	2.0–2.5	2550–2650
3	volcanics	2.0–3.5	2.5–3.0	2600–2800
4	Carpathian and Pannonian upper crust	1.0–3.5	2.0–3.0	2740–2750
5	European Platform upper crust	1.5–2.5	2.0–2.5	2650–2820
6	European Platform lower crust	0.2	2.0	2950–2980
7	Carpathian and Pannonian lower crust	0.2	2.0	2930
8	Carpathian and Pannonian mantle lithosphere	0.05	3.40	3200
9	European mantle lithosphere	0.05	3.40	3200
10	mantle lithosphere anomalous body	0.05	3.40	3210
11	main suture zone	0.1	2.50	3000

[a]No., reference number in Figure 3; HP, heat production ($\mu W/m^3$); TC, thermal conductivity (W/(m K)); ρ_0, density at room temperature (kg/m^3).

[9] Mid-Miocene back-arc extension in the Pannonian Basin area indicates subduction retreat [*Royden*, 1988], which is regarded as the main driving mechanism also for the Miocene motions of the two intra-Carpathian microplates Alcapa and Tisza-Dacia. These microplates moved independently with different directions and velocities, confined only by the Mesozoic geometry of this embayment [*Lankreijer et al.*, 1999] into which they moved. Rotations of the microplates are indicated by paleomagnetic data, which reveal an 80° counterclockwise rotation of the Alcapa microplate [e.g., *Kováč et al.*, 1997; *Márton and Fodor*, 1995] and a 60° clockwise rotation of the Tisza-Dacia microplate since early Miocene times [*Balla*, 1987; *Márton and Fodor*, 1995; *Linzer et al.*, 1998; *Panaiotu*, 1998; *Wortel and Spakman*, 2000; *Sperner et al.*, 2001; *Dupont-Nivet et al.*, 2005]. Both lithospheric fragments amalgamated at the end of early Miocene (Karpatian) along the mid-Hungarian tectonic zone [*Csontos*, 1995].

[10] The Neogene evolution of the Carpathian arc was driven by subduction of lithosphere underlying flysch basins, in three stages: (1) late Oligocene to early Miocene subduction of the remnant oceanic lithosphere of the internally situated Peninnic-Magura flysch zone basement [*Kováč et al.*, 1994], (2) late early Miocene to Sarmatian, and (3) Pannonian to Pliocene subduction of lithosphere underlying the externally situated Krosno-Moldavian flysch zone basement. The corresponding suture zone follows the subsurface contact of the European Platform with Carpathian elements. Its approximate position has being indicated by the axis of the Carpathian gravity low [*Tomek et al.*, 1989; *Tomek and Hall*, 1993].

[11] Continental collision started in the northernmost part of the Carpathians and later shifted toward the SE and S, leading to a corresponding shift of foreland basin depocenters [*Jiříček*, 1979; *Meulenkamp et al.*, 1996; *Kováč*, 2000; *Sperner et al.*, 2001] and shift of volcanic activity [*Pécskay et al.*, 1995; *Konečný et al.*, 2002; *Seghedi et al.*, 2004].

[12] The contrasting evolution of the accretionary prism and its final thrusting over foredeep sediments makes it possible to distinguish three segments with a different subduction history, roughly corresponding to the western Carpathians, northwestern part of eastern Carpathians, and southeastern part of eastern Carpathians [*Kováč*, 2000].

[13] The timing and spatial distribution of the arc-type (subduction-related) andesite volcanics indicate that subduction processes were halted when the subducting slab approached a near vertical position, followed closely in time by detachment of the sinking lithosphere slab from the continental margin. The slab detachment is indicated by the absence of intermediate-depth seismicity in the northern part of the Carpathians [*Sperner et al.*, 2001]. Similar to the evolution of collision in the northern Carpathians, slab detachment started in the north and propagated toward the south. Final detachment of the sinking lithosphere fragments in the eastern Carpathians is confirmed by results of seismic tomography [*Goes et al.*, 1999; *Wortel and Spakman*, 2000]. Lithosphere detachment in progress is indicated by the interpretation of the Vrancea seismic zone at the southern tip of the eastern Carpathians [*Constantinescu and Enescu*, 1964; *Sperner et al.*, 2001]. This zone is inferred to be the final expression of the progressive subduction, slab detachment and plate boundary retreat that were responsible for the evolution of the back-arc basin system [*Tomek and PANCARDI Colleagues*, 1996; *Seghedi et al.*, 1998; *Wortel and Spakman*, 2000].

[14] On the basis of seismic and gravity data, *Sperner et al.* [2004] proposed a model for the Tertiary evolution of the eastern-southern Carpathian junction that is consistent with evolution of the Transylvanian and Foscani basins and the dip angle of the slab. The model assumes Tertiary subduction, which started with a shallow dipping slab (evolution of the Transylvanian Basin on the overriding plate) followed by slab steeping and later delamination, so that the present-day position is subvertical and beneath the foredeep (evolution of Foscani Basin on the foreland).

[15] The generally short-lived volcanic activity of the arc-type (subduction-related) andesite volcanics is interpreted either as an indication of a limited width of the subducted lithosphere (300–200 km in the NW segment of the Krosno-Moldavian zone and less than 200 km in the SE segment of the zone) or as an indication of the progressive detachment of the sinking slab from the platform margin during the volcanic activity.

[16] The time lap of 8–10 Ma between the initial stage of subduction and onset of the arc type basaltic andesite to andesite volcanic activity along the Carpathian arc suggests an average subduction rate of 1.5–2.5 cm a year. This

estimate falls on the lower limit of rates (2–2.5 cm/year) derived by hydrodynamic model calculations [*Nur et al.*, 1993] for a microplate of oceanic lithosphere 70 km thick, 500 km wide, and 500 km long. The low subduction rate implies obstacles for the compensating asthenosphere flow, perhaps represented by confining thick lithosphere on the NW and SE sides of the arc (the Bohemian Massif and Moesian platform) [*Konečný et al.*, 2002].

[17] Subduction in the Outer Carpathian flysch basin was since its beginning compensated by asthenospheric mantle upwelling and related rifting in the back-arc realm. Spatial distribution and timing of back-arc basins reflected the segmentation of the sinking slab, as well as its final verticalization. This segmentation should be understood as a gravity driven process allowing for asthenospheric side flow to take place and hence to speed up gravity driven overturn (subduction).

[18] Thinned crust and lithosphere in the Pannonian region corresponds to the diapiric upwelling of asthenospheric mantle. The thinner lithosphere is documented by thermal modeling [e.g., *Lenkey*, 1999] and by the spatial distribution of the regional extension-related silicic and andesitic volcanism [*Szabó et al.*, 1992; *Kováč*, 2000; *Konečný et al.*, 2002]. Diapiric upwelling of asthenospheric mantle started in the west following subduction in front of the western Carpathians in early Miocene times, then continued toward the northeast following subduction in front of the NW part of the eastern Carpathians in early/middle Miocene times, and finally it affected the central and eastern regions during middle/late Miocene times following initiation of subduction in the front of the SE part of the eastern Carpathians.

[19] Late stage alkali basalt volcanics testify that during the late stage of back-arc basin evolution, extensional conditions persisted and that the diapiric uprise of asthenospheric mantle incorporated unmetasomatized mantle material, perhaps brought into the area by compensating asthenospheric mantle counterflows.

3. Method

[20] Since the link between surface heat flow values and geotherms in the deeper parts of the crust and in the upper mantle may be obscured by near-surface effects like groundwater flow or paleoclimatic variations as well as by the generally unknown distribution of heat-producing elements in the crust, determinations of lithospheric thickness based only on surface heat flow data have large uncertainties. To reduce this uncertainty, we take into account the dependence of density on temperature through the coefficient of thermal expansion:

$$\rho(T) = \rho_0(1 - \alpha(T - T_0))$$

where $\rho(T)$ is the density (kg/m^3) at a given temperature T(°C), ρ_0 is the density at temperature T_0 (usually room temperature except for the mantle, where it is given at asthenospheric temperature) and α is the thermal expansion coefficient taken as 3.5×10^{-5} K^{-1}.

[21] We constrain in this way lateral temperature variations through their effect on geophysical observations that are influenced by the density distribution. The geophysical observables used for this, topography, gravity and geoid, have all different distance dependence on density variations.

[22] The topography is calculated in local isostatic equilibrium using the formulas presented by *Lachenbruch and Morgan* [1990]:

$$h = \frac{\rho_a - \rho_L}{\rho_a} H + h_0$$

with h topography (m), ρ_a asthenospheric density (3200 kg/m^3), ρ_L average lithospheric density (kg/m^3), calculated along columns based on the defined bodies (see description below), H thickness of the lithosphere (m), and h_0 calibration constant (−2380 m) that refers the obtained topography to average mid-oceanic ridge topography [*Lachenbruch and Morgan*, 1990].

[23] If h becomes negative (labeled h_{neg}), one has to add the effect of water pressure:

$$h_{neg} = \frac{\rho_a}{\rho_a - \rho_{water}} h$$

Topography is therefore sensitive to lateral variations of the average density above a certain compensation level. This level is defined within the asthenosphere that is supposed to have a sufficiently small viscosity to relax shear stresses at geologically short timescales and to have a constant density. For the generally assumed relatively thin lithosphere of the Pannonian Basin, local equilibrium should be obtained for wavelengths above approximately 100 km.

[24] Gravity anomalies depend on distance r to density variations by r^{-2}. Therefore gravity anomalies will depend mainly on density variations within the crust with a relatively small, however not negligible, effect from density variations within the mantle. Gravity anomalies are calculated using a two-dimensional (2-D) algorithm [*Talwani et al.*, 1959].

[25] The geoid, reflecting variations of the elevation of the gravimetric isopotential surface corresponding to sea level depends on the distance to density variations by r^{-1}. The geoid is therefore more sensitive to near-surface density variations (specifically to topography) than to deep ones. However, the decay is relatively slow, and therefore geoid anomalies reflect crustal as well as mantle density variations. The formulas used have been published by *Zeyen et al.* [2005].

[26] The program used consists of a 2-D finite element algorithm to calculate the temperature distribution based on a user-defined lithospheric structure where each body is characterized by its density, thermal conductivity and heat production. The body structure is as much as possible constrained by existing seismic and geological data. The thermal boundary conditions are fixed temperatures at the upper limit (Earth's surface; 20°C) and the lower one (lithosphere-asthenosphere boundary; 1300°C) as well as no horizontal heat flow at the lateral, vertical boundaries.

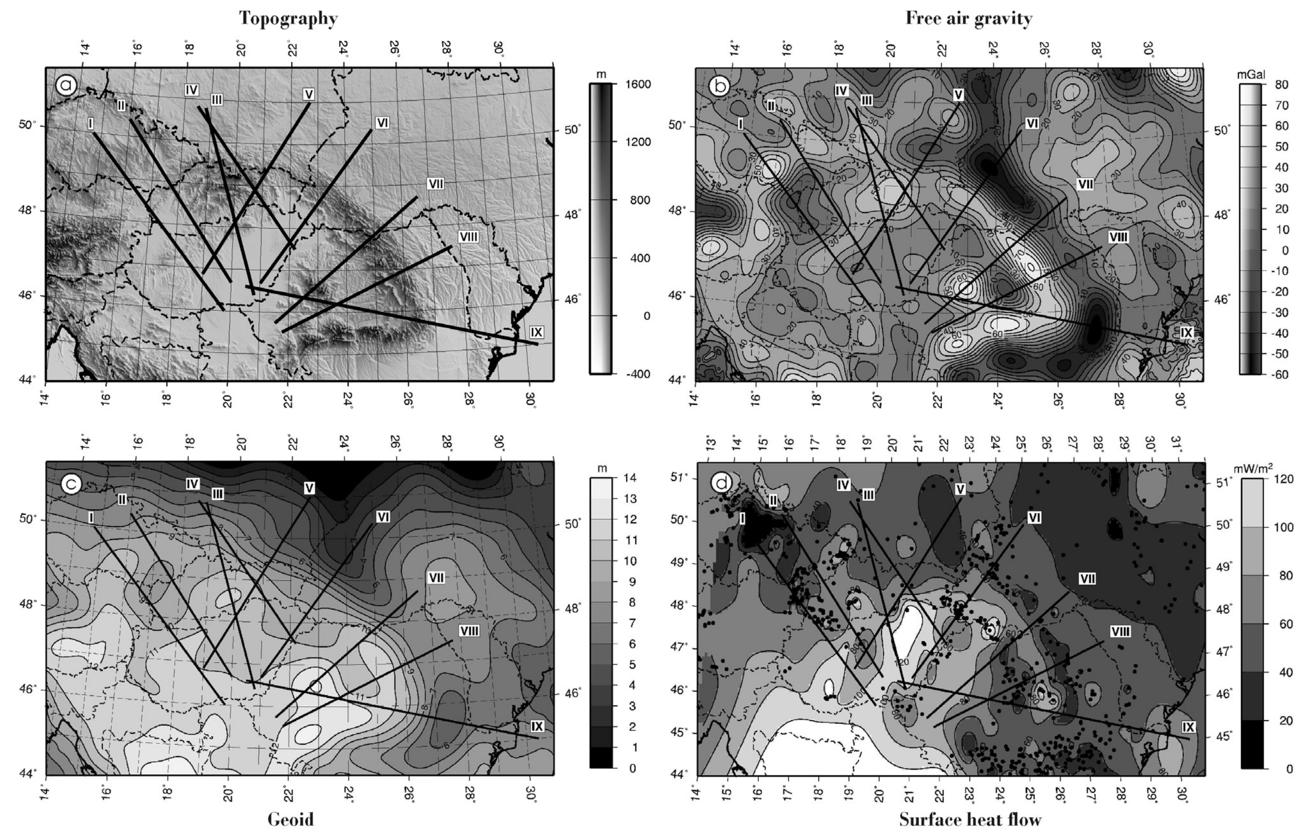

Figure 2. (a) Topography of the Carpathian-Pannonian Basin region (from GTOPO30 data set [*Gesch et al.*, 1999]). (b) Smoothed free-air gravity anomaly map of the Carpathian-Pannonian Basin region (from TOPEX gravity data, 1 min grid, ftp://topex.ucsd.edu/pub). Contour interval 10 mGal. (c) Geoid anomaly map of the Carpathian-Pannonian Basin region (from TOPEX geoid data, 2 min grid, ftp://topex.ucsd.edu/pub). Contour interval 1 m. (d) Map of the surface heat flow density of the Carpathians-Pannonian Basin region [from *Pollack et al.*, 1993]. Contour interval 20 m/W m^2.

After the calculation of the temperature distribution, the body densities are modified at each node of the finite element grid taking into account the thermal expansion coefficient. With this modified density distribution, we calculate the gravity and geoid variations and the topography, after having calculated the average lithospheric density for every column of the grid. Data and model results are compared and the model is then changed interactively by trial and error until an acceptable fit is obtained.

4. Eastern Carpathian Lithospheric Transects

[27] After having studied the lithospheric structure along five transects across the western Carpathians [*Zeyen et al.*, 2002], the present study concerns the structure of the eastern Carpathian lithosphere where the integrated modeling algorithm has been applied to four transects (Figure 1). Transects VI, VII, and VIII start in the Pannonian Basin and cross the orogen in NE direction to end on the European Platform. Transect VI passes through the Transcarpathian Basin whereas transects VII and VIII cross the Apuseni Mountains and the Transylvanian Basin. Transect IX (the Vrancea transect) crosses the Apuseni Mountains and the Transylvanian Basin and then passes through the seismogenic Vrancea zone.

4.1. Geophysical Data

[28] Topography (Figure 2a) has been taken from the GTOPO30 database [*Gesch et al.*, 1999] having estimated errors of less than 20 m (see, e.g.,http://www.ngdc.noaa.gov/mgg/topo/report/s7/s7Bi.html). The European Platform has an elevation of about 150–300 m, the eastern Carpathian foreland is characterized by an average topography of 550 m with a tendency of the peaks to increase from 700 m (transect VI) to 900 m (transects VIII and IX). The Carpathian Mountains have an average elevation of 1000 m, the maximum of about 1200 m being encountered along transects VII and VIII. Minimum elevations occur in the Pannonian Basin (approximately 100 m). Average topography in the Pannonian Basin is about 150 m.

[29] The free air gravity anomalies (Figure 2b) were taken from the TOPEX 1-min gravity data set (ftp://topex.ucsd.edu/pub [*Sandwell and Smith*, 1997]). Values between −50 and +75 mGal are observed with uncertainties of approximately 3–5 mGal. The free air anomalies reflect in general a smoothed topography. The largest amplitudes of

+70 mGal are found in the higher regions of the central eastern and southern Carpathians with another, though slightly less important maximum in the Apuseni Mountains. They are bordered by relative minima in the foreland basins and in the Pannonian Basin (mainly in the Transylvanian Basin). A more detailed analysis shows that the anomalies in the Pannonian Basin are, in relation to the topographic elevation, less pronounced than those of the different foreland basins and the Transylvanian Basin pointing toward shallower density variations. The lowest amplitudes of −50 mGal occur in the Ukrainian and Romanian (Vrancea) foreland.

[30] Geoid data (Figure 2c) are taken from the EGM96 global model [*Lemoine et al.*, 1998] with errors of less than 30 cm (http://cddis.gsfc.nasa.gov/926/egm96/contents.html). In order to avoid effects of sublithospheric density variations on the geoid, we have removed the geoid signature corresponding to the spherical harmonics developed until degree and order 8 [*Bowin*, 1991]. Most of the Carpathian-Pannonian region stands out as positive anomaly with maxima of near 14 m in the southern Carpathians and the Apuseni Mountains. Also the eastern Carpathians have a positive signature, whereas the northern part of the western and eastern Carpathian junction (transect VI) and the Transylvanian Basin as well as the European Platform show intermediate values. Relative minima are located along the foreland basin.

[31] The surface heat flow data (Figure 2d) were compiled from the worldwide data set of *Pollack et al.* [1993] and the maps of heat flow of the western Carpathians and their vicinity published by *Čermák et al.* [1992], *Král* [1995], *Šefara et al.* [1996], *Gordienko and Zavgorodnyaya* [1996], *Majorowicz* [2004], and *Lenkey* [1999]. The dominant feature of the heat flow map is an increase from the European Platform via the Carpathians toward the Pannonian Basin. The heat flow in the European Platform varies from 10 to 70 mW/m^2. In the outer eastern Carpathians the average heat flow increases from values of 40 mW/m^2 to about 60 mW/m^2. The Pannonian Basin is characterized by the highest mean values (90 mW/m^2), attaining over 110 mW/m^2 in the northeastern part of this basin. Neogene volcanic areas of the western and eastern Carpathians attain the largest values up to 120 mW/m^2.

[32] The thickness of the outer Carpathian foredeep sediments was compiled using data published by *Tomek et al.* [1987, 1989], *Poprawa and Nemčok* [1989], *Krejčí and Jurová* [1997], *Kováč* [2000], *Matenco* [1997] and *Cornea et al.* [1981]. The model of the outer Carpathian Flysch belt sediments was obtained using data from *Krejčí and Jurová* [1997], *Poprawa and Nemčok* [1989], *Poprawa et al.* [2002], *Mocanu and Radulescu* [1994], *Matenco* [1997], *Kováč* [2000] and *Sandulescu* [1994]. The maps of the pre-Tertiary substratum relief in the inner Carpathian-Pannonian Basin region published by *Bielik* [1988] and *Kilényi et al.* [1989] give a good indication of the sediment thickness. In the Pannonian Basin, the Neogene sediments are about 2–3 km thick, reaching in some subbasins more than 6 km and in the Danube Basin over 9 km.

[33] The depth of the boundary between upper and lower crust varies between 17 and 21 km. The deepest part of this boundary has been interpreted beneath the Pienniny Klippen belt [*Bielik et al.*, 1990a, 1990b]. For the input depth of the Moho discontinuity we used the maps published by *Mayerová et al.* [1994], *Šefara et al.* [1996], *Horváth* [1993], *Lenkey* [1999], *Guterch et al.* [1986], and *Lazarescu et al.* [1983]. The Carpathian mountain belt is characterized by a thicker crust (30–55 km) in comparison with thinner crust (25–30 km) in the Pannonian Basin. The Moho depth increases to 45–50 km underneath the Tornquist-Teisseyre zone [e.g., *CELEBRATION 2000 Working Group*, 2000]. The crustal thickness tends to increase from west to east along strike of the Carpathian orogen. The western Carpathians are characterized by a crustal thicknesses of about 30–35 km, the eastern Carpathians by 32–42 km and the seismogenic Vrancea zone by up to 55 km. The Moho underneath the southern Carpathians is at a depth of 42–50 km. However, in general, the Carpathians are characterized by a rather thin crust in comparison with other orogens.

[34] An initial model of the lithosphere thickness was defined from maps published by *Babuška et al.* [1988], *Horváth* [1993], *Šefara et al.* [1996], and *Mocanu and Radulescu* [1994].

[35] For the different transects we extracted the data from the mentioned data sets along a strip 50 km to each side of the transects (100 km for the heat flow data) in order to have some measure of the 3-D variability of the input data. These data are shown in Figure 3 as dots with uncertainty bars which indicate the 1σ deviation within the mentioned strip. For the surface heat flow data, in some areas no standard deviations could be calculated due to the low density of measurement points (Figure 2d). In those cases, we assumed uncertainties of 10 mW/m^2 (i.e., 10–20%). In most areas, the gravity uncertainties are less than ±10 mGal and geoid uncertainties less than ±0.5 m, indicating that the third dimension does not have a crucial influence in the modeling. The topography varies very little in the foreland and in the Pannonian Basin. In the mountain areas of the eastern Carpathians and Apuseni Mountains, however, the variations are much larger and the interpretation is therefore less straightforward. Nevertheless, taking an average height is probably a good guess, since the strong short-wavelength topography variations between mountains and valleys can never be considered as compensated locally. Taking into account that "local isostasy" is a simplifying assumption, we opted in the case of incompatibility between gravity and

Figure 3. Lithospheric models For all models, I, surface heat flow; II, Free-air gravity anomaly; III, geoid; IV, topography with dots corresponding to measured data with uncertainty bars and solid lines to calculated values; V, lithospheric structures; Shadings are 1, sediments; 2, upper crust; 3, lower crust. In the lithospheric mantle, isotherms are indicated every 200°C. Numbers within the model bodies correspond to material number in Table 1. Numbers on top of the figures indicate the starting and endpoint coordinates of the profiles. The dots in transect IX represent ISC hypocenters (1970–2005; $M_w \geq 4$) projected from a strip of 50 km to each side of the profile [*International Seismological Centre* (ISC), 2001].

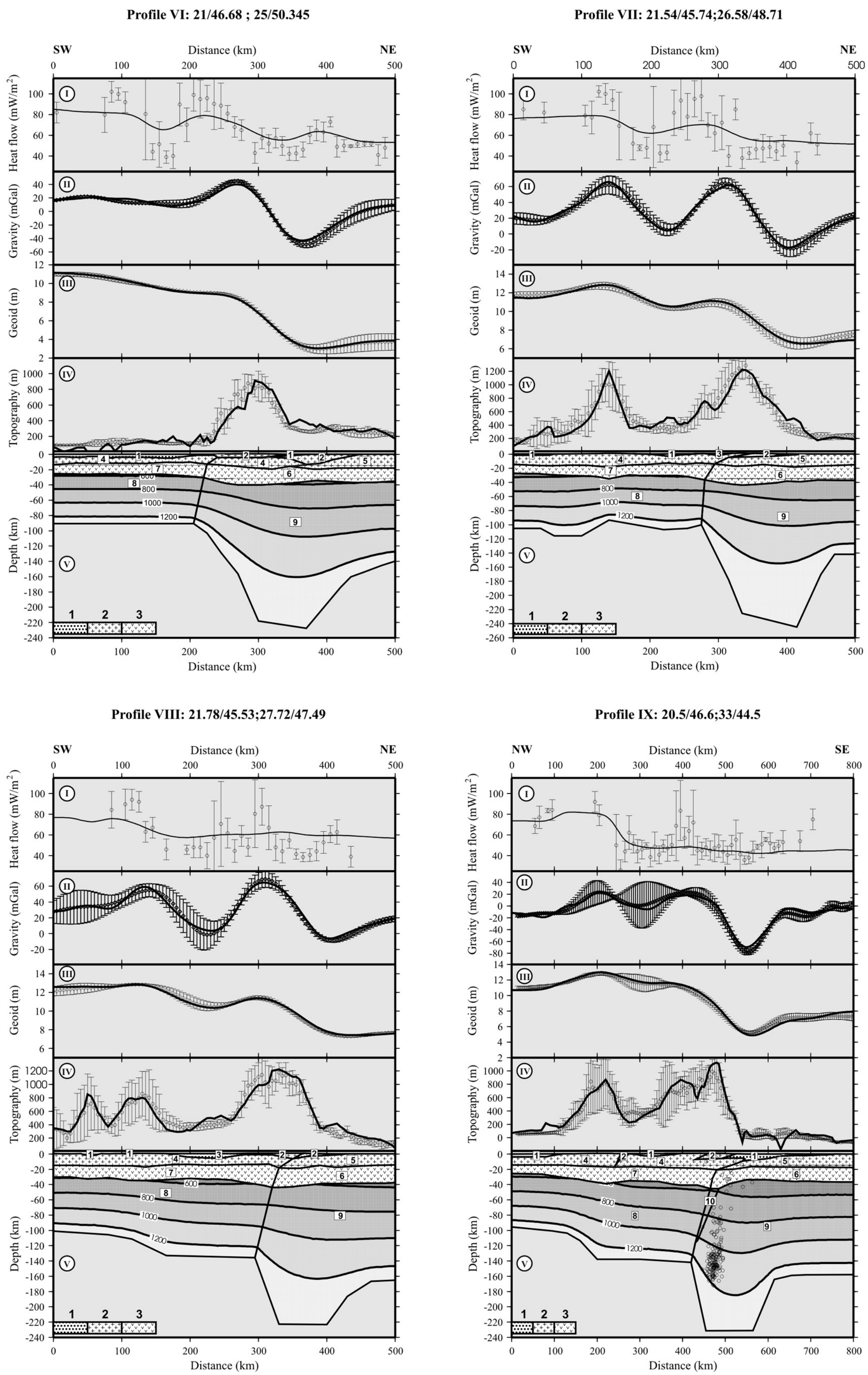
Profile VI: 21/46.68 ; 25/50.345
Profile VII: 21.54/45.74;26.58/48.71
Profile VIII: 21.78/45.53;27.72/47.49
Profile IX: 20.5/46.6;33/44.5
Distance (km)
Heat flow (mW/m²)
Gravity (mGal)
Geoid (m)
Topography (m)
Depth (km)
SW
NE
NW
SE

Figure 3

geoid data on the one hand and topography data on the other hand for giving preference to fitting the gravity and geoid anomalies.

4.2. Modeling Results

[36] On the basis of the geophysical data mentioned above we constructed initial density models. The thermal and density-related parameters were then modified by trial and error until a reasonable fit was obtained between data and model predictions (Figure 3). The final densities and thermal parameters are given in Table 1. The misfit in the free air anomalies is generally smaller than the uncertainty bars. The short wavelengths of the discrepancies suggest that they are due to shallow and small-scale crustal structures that could not be considered in these regional models. Misfits of short wavelength are also visible in the topography data and correspond to local features such as thrusting structures of the eastern Carpathians, which are probably not compensated by local isostasy and cannot be reproduced by the models. The heat flow data show a high degree of scatter. Generally, it is due to groundwater circulation or paleoclimatic effects [*Kukkonen et al.*, 1993; *Stulc*, 1998]. Since these effects are not included in the used algorithm, our models result in a smooth variation with a minimum of 50 mW/m^2 in the European Platform and a maximum of about 90 mW/m^2 in the Pannonian Basin.

[37] A general feature of the lithosphere thickness in the study region is its increase from the youngest and hottest area of the Pannonian Basin to the oldest and coolest area of the European Platform. The lithospheric thickness underneath the European Platform increases slightly in our models from about 140 km in the NW (transects VI and VII) to about 160 km in the SE (transects VIII and IX). The Pannonian Basin is characterized by a ca. 90 km thick lithosphere (transects VI and IX) increasing southward to about 110 km (transects VII and VIII). This thickness is larger than published earlier [e.g., *Horváth*, 1993; *Lenkey*, 1999]. Therefore part of the surface heat flow has to be explained by an increase in radioactive heat production in the Pannonian upper crust and sediments. However, reducing the lithospheric thickness to the published values between 40 and 60 km would uplift considerably the modeled topography, making it incompatible with the observed one. The lithosphere thickness underneath the Transylvanian Basin reaches in the models about 100 to 130 km. Underneath the Apuseni Mountains the lithosphere thickness increases to 90–130 km.

[38] The most interesting feature can be seen underneath the eastern Carpathians and their foreland. Our models show along all transects a strong lithospheric thickening to more than 220 km. This large thickening is needed to obtain a good correlation between the observed and modeled topography and geoid anomalies. In the seismogenic area of Vrancea (profile IX), we have projected the ISC hypocenters from a 50 km wide strip to both sides of the profile onto Figure 3 (bottom right). These hypocenter locations coincide well with the western limit of the thickened lithosphere which corresponds well to the seismic tomography models [*Sperner et al.*, 2001] where those hypocenters are related to the upper limit of a near-vertical subducting slab.

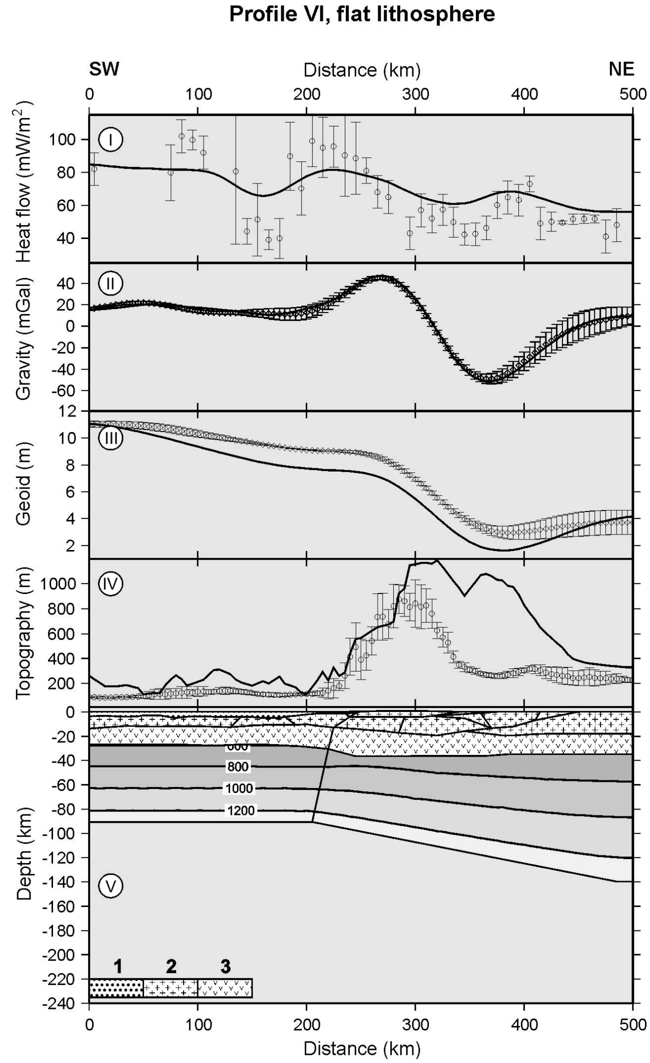

Figure 4. Modified model for profile VI for illustration of the effect of lithospheric thickening on the different data. The base of the lithosphere has been flattened in order to eliminate the strong thickening but maintaining the general thickness increase from the Pannonian Basin to the European Platform. The crustal thickness and density distribution have been changed so that the model fits the gravity data.

[39] Figure 4 shows an example for the sensitivity of the model. We eliminated the strong thickening underneath transect VI and changed the crustal structure and densities in order to fit the gravity data. Now, it is evident, that it is possible to fit the gravity data only with variations at crustal level; however, the other data, especially topography are then no longer explained. This example shows the importance of taking into account different data sets for modeling of lithospheric structures.

[40] Thickening of the lithosphere in the eastern Carpathian foreland is only accompanied by small crustal thick-

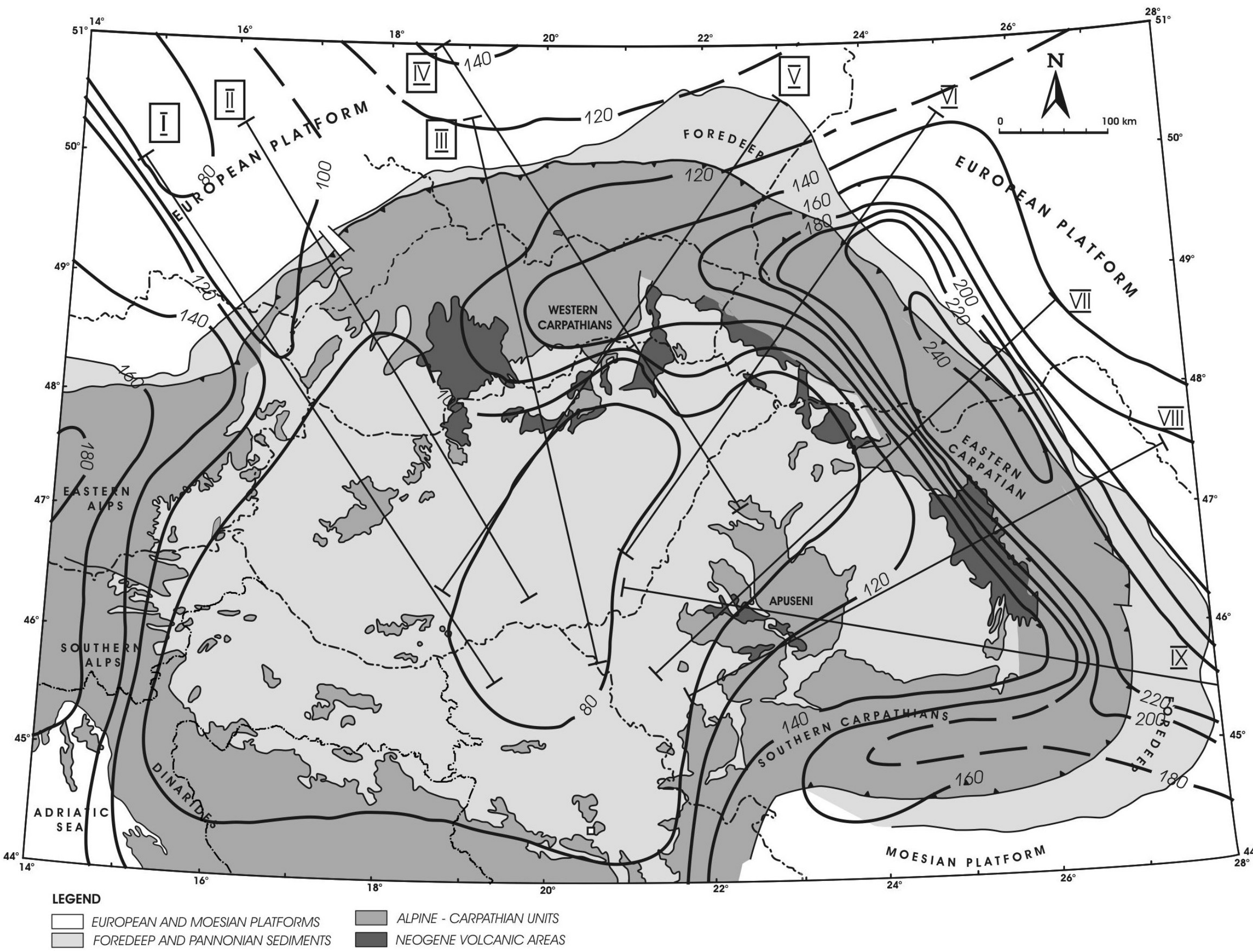

Figure 5. Lithosphere thickness map of the Carpathian-Pannonian Basin region (compiled after the results presented here and results published earlier by *Zeyen et al.* [2002], *Babuška et al.* [1988], *Horváth* [1993], and *Lenkey* [1999]).

ening, except for the Vrancea zone (transect IX). On all transects, the crustal thickening is shifted southwestward with respect to the lithosphere thickening toward the areas of highest topography in the central (inner) eastern Carpathians. In the Vrancea area, models based on seismic data are contradictive: *Mocanu and Radulescu* [1994] indicate a crustal thickening to nearly 50 km, whereas *Hauser et al.* [2001] and *Landes et al.* [2004] give a maximum thickness of 40–41 km. In order to fit gravity and geoid data, we have to model a local thickening underneath the mountain chain to an intermediate thickness of 45 km. Also a model with a slightly thinner crust could still fit the data. On all transects, crustal thickness beneath the European Platform is rather constant around 37–38 km. Under the Pannonian Basin, the crust thins to 26–27 km with a clear increase underneath the Apuseni Mountains to more than 35 km.

[41] Since the method used is a trial and error method, we calculated a large number of models before finding the ones presented here. This allows us to estimate the uncertainty of the lithospheric thickness to about 10–15%, i.e., in most parts of the model about 10–15 km. In the thickened areas the lithosphere may be some 20 km thinner. However, the thickness may be considerably larger, since the method looses resolution if a structure becomes much thicker than wide at the base of the lithosphere. So, we consider the thickening as significant, but we cannot give a maximum estimate (e.g., in the Vrancea zone).

5. Discussion and Conclusions

[42] Joint modeling of surface heat flow, gravimetric and topographic data, using geological and crustal seismic data as constraints, allowed us to establish a new model of the lithospheric structure of the Carpathians and parts of their surrounding tectonic units. Taking into account all our results obtained along nine transects (transects I, II, III, IV and V from *Zeyen et al.* [2002] and transects VI, VII, VIII and IX presented here) we made a new map of the lithosphere in the Carpathian-Pannonian Basin region, which is illustrated in Figure 5. The resultant map is a compilation of our results and partly the results published

earlier by *Babuška et al.* [1988], *Horváth* [1993], and *Lenkey* [1999].

[43] This map shows important variations in lithospheric thickness across the chain as well as along strike of the Carpathians arc. It can be observed that the lithosphere thickness increases along the strike of the Carpathians from the western to the eastern Carpathians. Under the western segment of the western Carpathians (in the transition zone to the eastern Alps), no lithospheric thickening is observed. The values vary from 100 to 120 km. In the Miocene, the Alpine-Carpathian-Pannonian (Alcapa) lithosphere fragment moved toward the east along the left-lateral strike-slip Salzachtal-Ennstal-Mariazell-Puchberg fault zone in the eastern Alps and along the similar Mur-Mürz-Leitha fault zone toward the northeast at the Alpine–Carpathian boundary [*Ratschbacher et al.*, 1991a, 1991b; *Fodor*, 1995; *Linzer*, 1996; *Lankreijer et al.*, 1999]. This means that the relative movement of the Alcapa lithosphere fragment changed from E to NE as a result of lateral extrusion into the open ''Carpathian bay''. This scenario could explain the absence of lithosphere thickening in the transition between Alps and Carpathians since the movement was mainly strike-slip along a deep reaching fault following the contact of the Bohemian Massif and the western Carpathians.

[44] Lithosphere thickness starts to increase in the eastern segment of the western Carpathians (up to 150 km), and reaches a maximum value of 240 km in the eastern Carpathians and in the Ukrainian and Romanian foreland. This thickening is interpreted as remnants of a slab, which started to break off in the Miocene. Our results are in good agreement with the results of seismic tomography by *Spakman* [1990], *Spakman et al.* [1993], *Goes et al.* [1999], and *Wortel and Spakman* [2000]. They also suggest remnants of deep subduction and slab detachment below the Carpathian-Pannonian Basin region. They showed that the slab seems to be detached from the European plate (probably except for the seismogenic Vrancea zone and the southeastern Carpathians). A flat-lying, high-velocity anomaly at the bottom of the upper mantle has been interpreted as subducted lithosphere that sunk into the deeper mantle as a result of rollback and slab detachment along strike of the Carpathian arc. This important roll-back could also explain why crustal thickening is not observed above the slab or even behind it with respect to the direction of subduction, but in front of it. The increasing thickness of the lithospheric slab from the western Carpathians to the eastern Carpathians supports the suggestion that the slab break-off started in the NW and propagated toward the SE, the seismogenic Vrancea zone being inferred as the final expression of the progressive subduction, slab roll-back and plate boundary retreat that were responsible for the evolution of the arc [*Tomek and PANCARDI Colleagues*, 1996; *Kazmer et al.*, 2003].

[45] The lithosphere under the Pannonian Basin resulting from our models is thicker than usually supposed. Our models do not support a thinning to less than about 70 km. Indications for extreme thinning of the lithosphere to only 40 km [*Ádám and Bielik*, 1998] may be local features under a few narrow subbasins, not detected on our profiles. However, the regional difference of 10–20 km, although not far from the estimated uncertainties of our models, may be significant. Different hypotheses may be put forward to explain this difference. The simplest would be that seismic, magnetotelluric and thermal analyses do not see the same variations of physical properties and that therefore different methods give the lithosphere-asthenosphere boundary at different temperatures. On the other hand, it is claimed that the alkaline volcanism trace elements show a less depleted uppermost mantle than normal [e.g., *Rosenbaum et al.*, 1997]. Our models show mainly that the lower lithosphere has to be denser than a normal lithosphere of 60 km thickness. We interpret this higher density by lower temperatures; however, it could be also due to less depleted, possibly plume-related material. Nevertheless, in order for this argument to be valid, the less depleted material should not form the asthenosphere, in which case the average density of the lithosphere would have to be even larger in order to explain the observed low elevation.

[46] To summarize, we present here a study that allows to image with relatively good resolution the variations of lithosphere thickness along the Carpathian chain from the transition to the Alps in the NW to the Vrancea zone in the SE. The results correspond well to the geodynamic ideas concerning the evolution of the slab that is supposed to have broken off and sunk into the asthenosphere during time, starting in the NW about 15 Ma ago and still being attached to the overlying lithosphere in the Vrancea zone. This is reflected by an increasing thickness of the lithosphere toward the regions of recent break-off. Where high-resolution seismic data are available, the model shows similar features (Vrancea zone). In other areas, low-resolution large-scale tomographic models are complemented by our models with more details within the lithosphere. As a corollary, we obtained new values for the lithospheric thickness in the Pannonian Basin that are some 20 km larger than thicknesses predicted by other authors. If this result is accepted, it could mean that on the scale of the whole basin the back-arc thinning is less important than supposed. It could, however, also be interpreted as an effect of less depleted, plume-related lithosphere.

[47] **Acknowledgments.** Bielik and Dererová are grateful to the Slovak Grant Agency VEGA (projects 2/3004/23, 2/3057/23) and to the Science and Technology Assistance Agency (project APVT-51-002804) for the support of this work. We thank B. Sperner and F. Neubauer and an anonymous Associate Editor for the constructive and helpful reviews.

References

Ádám, A. (1976), The Transdanubian crustal conductivity anomaly, *Acta Geod. Geophys. Mont. Hung.*, *12*, 73–79.

Ádám, A. (1996), Regional magnetotelluric (MT) anisotropy in the Pannonian basin (Hungary), *Acta Geod. Geophys. Hung.*, *31*, 191–216.

Ádám, A., and M. Bielik (1998), The crustal and upper-mantle geophysical signature of narrow continental rifts in the Pannonian basin, *Geophys.*

J. Int., *134*, 157–171, doi:10.1046/j.1365-246x.1998.00544.x.

Babuška, V., J. Plomerová, and J. Šílený (1987), Structural model of the subcrustal lithosphere in central Europe, in *Composition, Structure and Evolution of the Lithosphere-Asthenosphere System*, *Geodyn. Ser.*, vol. 16, edited by K. Fuchs and C. Froidevaux, pp. 239–251, AGU, Washington, D. C.

Babuška, V., J. Plomerová, and P. Pajdušák (1988), Lithosphere-asthenosphere in central Europe: Models derived from P residuals, paper presented at 4th EGT Workshop: The Upper Mantle, Comm. of the Eur. Commun., Eur. Sci. Found., Utrecht, Netherlands.

Balla, Z. (1987), Tertiary paleomagnetic data for the Carpatho-Pannonian region in the light of Miocene rotation kinematics, *Tectonophysics*, *139*, 67–98.

Bielik, M. (1988), A preliminary stripped gravity map of the Pannonian Basin, *Phys. Earth Planet. Inter.*, *51*, 185–189.

Bielik, M., O. Fusán, M. Burda, M. Hubner, and V. Vyskocil (1990a), Density models of the western Carpathians, *Contrib. Geophys. Inst. Slov. Acad. Sci.*, *20*, 103–113.

Bielik, M., D. Majcin, O. Fusán, M. Burda, V. Vyskocil, and J. Trešl (1990b), Density and geothermal modelling of the western Carpathian Earth's crust, *Geol. Carpathians*, *42*, 315–322.

Bowin, C. (1991), The Earth's gravity field and plate tectonics, *Tectonophysics*, *187*, 69–89.

CELEBRATION 2000 Working Group (2000), Contrasts of lithospheric structures in the TESZ (from NW to SE Poland) along TTZ and CEL03 seismic profiles, *Geol. Carpathians* [CD-ROM], *53*.

Čermák, V. (1982), Regional pattern of the lithosphere thickness in Europe, in *Geothermics and Geothermal Energy*, edited by V. Čermák and R. Haenel, pp. 1–10, Schweizerbarth, Stuttgart, Germany.

Čermák, V. (1994), Results of heat flow studies in Czechoslovakia, in *Crustal Structure of the Bohemian Massif and the West Carpathians*, edited by V. Bucha and M. Blíkovský, pp. 85–118, Springer, New York.

Čermák, V., M. Král, J. Kubík, J. Šafanda, M. Krešl, L. Kuferová, J. Jancí, I. Lizon, and I. Marušiak (1992), Subsurface temperature and heat flow density maps on the territory of the Czechoslovakia, in *Geothermal Atlas of Europe*, edited by E. Hurtig and V. Èermak, pp. 21–24, Herman Haack, Gotha, Germany.

Constantinescu, L., and D. Enescu (1964), Fault-plane solutions for some Roumanian earthquakes and their seismotectonic implication, *J. Geophys. Res.*, *69*, 667–674.

Cornea, L., F. Radulescu, A. Pompilian, and A. Sava (1981), Deep seismic soundings in Romania, *Pure Appl. Geophys.*, *119*, 1144–1165.

Csontos, L. (1995), Tertiary tectonic evolution of the intra-Carpathian area: A review, *Acta Vulcanol.*, *7*, 1–13.

Csontos, L., A. Nagymarosy, F. Horváth, and M. Kováč (1992), Tertiary evolution of the Intra-Carpathian area: A model, *Tectonophysics*, *208*, 221–241.

Dupont-Nivet, G., I. Vasiliev, C. G. Langereis, W. Krijgsman, and C. Panaiotu (2005), Neogene tectonic evolution of the southern and eastern Carpathians constrained by paleomagnetism, *Earth Planet. Sci. Lett.*, *236*, 374–387, doi:10.1016/j.epsl.2005.04.030.

Fodor, L. (1995), From transpression to transtension: Oligocene-Miocene structural evolution of the Vienna basin and the east Alpine-western Carpathian junction, *Tectonophysics*, *242*, 151–182.

Gesch, D. B., K. L. Verdin, and S. K. Greenlee (1999), New land surface digital elevation model covers the Earth, *Eos Trans. AGU*, *80*, 69–70.

Goes, S., W. Spakman, and H. Bijwaard (1999), A lower mantle source for central European volcanism, *Science*, *286*, 1928–1931.

Gordienko, V. V., and O. V. Zavgorodnyaya (1996), Estimation of heat flow in Poland, *Acta Geophys. Pol.*, *44*, 173–180.

Guterch, A., M. Grad, R. Materzok, E. Perchuč, and S. Toporkiewicz (1986), Results of seismic crustal studies in Poland (in Polish with English summary), *Publ. Inst. Geophys. Pol. Acad. Sci.*, *A-17*(192), 84–89.

Hauser, F., V. Raileanu, W. Fielitz, A. Bala, C. Prodehl, G. Polonic, and A. Schulze (2001), VRANCEA99—The crustal structure beneath the southeastern Carpathians and the Moesian Platform from a seismic refraction profile in Romania, *Tectonophysics*, *340*, 233–256, doi:10.1016/S0040-1951(01)00195-0.

Horváth, F. (1993), Towards a mechanical model for the formation of the Pannonian Basin, *Tectonophysics*, *226*, 333–357.

International Seismological Centre (ISC) (2001), Online bulletin, http://www.isc.ac.uk/Bull, Thatcham, U.K.

Jiříček, R. (1979), Tektogenetický vývoj karpatského oblúku behem oligocénu a neogénu, in *Tektonické Profily Západných Karpát*, edited by M. Mahel, pp. 205–214, GÚDŠ, Bratislava, Slovakia.

Kazmer, M., I. Dunkl, W. Frisch, J. Kuhlemann, and P. Ozsvart (2003), The Palaeogene forearc basin of the eastern Alps and western Carpathians: Subduction erosion and basin evolution, *J. Geol. Soc. London*, *160*, 413–428.

Kilényi, E., J. Šefara, A. Kröll, P. Steinhauser, F. Weber, D. Obernauer, L. Pospíšil, A. Šutora, J. Rumpler, and Z. Szabo (1989), Pre-Tertiary basement contour map of the Carpathian Basin beneath Austria, Czechoslovakia and Hungary, Eötvös Lórand Geofiz. Intezet, Budapest.

Konečný, V., M. Kováč, J. Lexa, and J. Šefara (2002), Neogene evolution of the Carpatho-Pannonian region: An interplay of subduction and back-arc diapiric uprise in the mantle, in *Neotectonics and Seismicity of the Pannonian Basin and Surrounding Orogens. A Memoire on the Pannonian Basin*, edited by F. Horváth, S. Cloetingh and G. Bada, pp. 165–194, Eur. Geophys. Soc., Strasbourg, France.

Kováč, M. (2000), *Geodynamický, paleografický a štruktúrny vývoj karpatsko-panónskeho regiónu v miocéne* (in Slovak), 202 pp., Veda Bratislava, Bratislava, Slovakia.

Kováč, M., J. Král, E. Márton, D. Plašienka, and P. Uher (1994), Alpine uplift history of the central western Carpathians: Geochronological, paleomagnetic, sedimentary and structural data, *Geol. Carp.*, *45*, 83–96.

Kováč, M., M. Bielik, J. Lexa, M. Pereszl'enyi, J. Šefara, I. Túnyi, and D. Vass (1997), The western Carpathian intramountane basins, in *Geological Evolution of the Western Carpathians*, edited by P. Grecula, D. Hovorka, and M. Putiš, pp. 43–64, Miner. Slovaca Corp.-Geocomplex, Geofyz. Bratislava and Geol. Surv. of Slovak Republic, Bratislava.

Kováč, M., A. Nagymarosy, N. Oszczypko, A. Slaczka, L. Csontos, M. Marunteanu, L. Matenco, and M. Márton (1998), Palinspatic reconstruction of the Carpathian-Pannonian region during the Miocene, in *Geodynamic development of the Western Carpathians*, edited by M. Rákus, pp. 189–217, Geol. Surv. Slovak Republic, Bratislava.

Král, M. (1995), Geothermal maps of Slovakia, in *Atlas of geothermal energy of Slovakia*, edited by O. Franko, A. Remšík, and M. Fendek, p. 125, GÚDŠ, Bratislava, Slovakia.

Krejčí, O., and Z. Jurová (1997), Structural map of the basement of the Flysch nappe sediments, Czech Géol. Surv., Brno, Czech Republic.

Kukkonen, I. T., V. Čermák, and E. Hurtig (1993), Vertical variation of heat flow density in the continental crust, *Terra Nova*, *5*, 389–398.

Lachenbruch, A. H., and P. Morgan (1990), Continental extension, magmatism and elevation; formal relations and rules of thumb, *Tectonophysics*, *174*, 39–62.

Landes, M., W. Fielitz, F. Hauser, and M. Popa (2004), 3-D upper crustal tomographic structure across the Vrancea seismic zone, *Romania, Tectonophysics*, *382*, 85–102, doi:10.1016/j.tecto.2003.11.013.

Lankreijer, A., M. Bielik, S. Cloetingh, and D. Majcin (1999), Rheology predictions across the western Carpathians, Bohemian Massif and the Pannonian Basin: Implications for tectonic scenarios, *Tectonics*, *18*, 1139–1153.

Lazarescu, V., L. Cornea, F. Radulescu, and M. Popescu (1983), Moho surface and recent crustal movements in Romania, Geodynamic connections, *Ann. Inst. Geol. Geofiz.*, *63*, 83–91.

Lemoine, F. G., et al. (1998), The development of the Joint NASA GSFC and NIMA geopotential model EGM96, NASA Goddard Space Flight Center, Greenbelt, Md.

Lenkey, L. (1999), Geothermics of the Pannonian Basin and its bearing on the tectonics of basin evolution, Ph.D. thesis, 215 pp, Free Univ., Amsterdam.

Lillie, R. J., M. Bielik, V. Babuška, and J. Plomerová (1994), Gravity modelling of the lithosphere in the eastern Alpine-western Carpathian-Pannonian Basin region, *Tectonophysics*, *231*, 215–235.

Linzer, H.-G. (1996), Kinematics of retreating subduction along the Carpathian arc, Romania, *Geology*, *24*, 167–170.

Linzer, H.-G., W. Frisch, P. Zweigel, R. Girbacea, H.-P. Hann, and F. Moser (1998), Kinematic evolution of the Romanian Carpathians, *Tectonophysics*, *297*, 133–156, doi:10.1016/S0040-1951(98)00166-8.

Majcin, D. (1994), Thermal state of west Carpathian Lithosphere, *Stud. Geophys. Geod.*, *4*, 345–364.

Majcin, D., V. Dudášová, and V. A. Tsvyashchenko (1998), Tectonics and temperature field along the Carpathian profile 2T, *Contrib. Geophys. Geod.*, *28*, 107–114.

Majorowicz, J. A. (2004), Thermal lithosphere across the Trans-European Suture Zone in Poland, *Geol. Q.*, *48*, 1–13.

Márton, E., and L. Fodor (1995), Combination of paleomagnetic and stress data–a case study from north Hungary, *Tectonophysics*, *242*, 99–114.

Matenco, L. C. (1997), Tectonic evolution of the outer Romanian Carpathians. Constraints from kinematic analysis and flexural modeling, Ph.D. thesis, 160 pp, Vrije Univ., Amsterdam.

Mayerová, M., M. Novotný, and M. Fejfar (1994), Deep seismic sounding in Czechoslovakia, in *Crustal Structure of the Bohemian Massif and the West Carpathians*, edited by V. Bucha and M. Blížkovský, pp. 13–20, Springer, New York.

Meulenkamp, J. E., M. Kováč, and I. Cícha (1996), On late Oligocene to Pliocene depocentre migrations and the evolution of the Carpathian-Pannonian system, *Tectonophysics*, *266*, 301–317.

Mocanu, V., and F. Radulescu (1994), Geophysical features of the Romanian territory, in *ALCAPA II, Geological Evolution of the Alpine-Carpathian-Pannonian System*, edited by T. Berza, *Rom. J. Tect. Reg. Geol.*, *75*, 17–36.

Nur, A., J. Dvorkin, G. Mavko, and Z. Ben-Avraham (1993), Speculations on the origins and fate of back arc basins, *Ann. Geofis.*, *36*, 155–163.

Panaiotu, C. (1998), Paleomagnetic constraints on the geodynamic history of Romania, *Monograph of Southern Carpathians*, *Rep. Geod. 7*, pp. 49–71, Warsaw Inst. of Technol., Warsaw.

Pécskay, Z., et al. (1995), Space and time distribution of Neogene and Quarternary volcanism in the Carpatho-Pannonian Region, *Acta Vulcanol.*, *7*, 15–28.

Pollack, H. N., S. J. Hurter, and J. R. Johnson (1993), Heat flow from the Earth's interior: Analysis of the global data set, *Rev. Geophys.*, *31*, 267–280.

Poprawa, D., and J. Nemčok (1989), *Geological Atlas of the Western Outer Carpathians and Their Foreland*, GUDŠ, Bratislava, Slovakia.

Poprawa, D., T. Malata, and N. Oszczypko (2002), Tectonic evolution of the Polish part of Outer Carpathian sedimentary basins: Constraints from subsidence analysis, *Prz. Geol.*, *30*, 1092–1108.

Praus, O., J. Pecová, V. Petr, V. Babuška, and J. Plomerová (1990), Magnetotelluric and seismological determination of lithosphere-asthenosphere transition in central Europe, *Phys. Earth Planet. Inter.*, *60*, 212–228.

Ratschbacher, L., O. Merle, P. Davy, and P. Cobbold (1991a), Lateral extrusion in the eastern Alps: 1. Boundary conditions and experiments scaled for gravity, *Tectonics*, *10*, 245–256.

Ratschbacher, L., W. Frisch, H. G. Linzer, and O. Merle (1991b), Lateral extrusion in the eastern Alps: 2. Structural analysis, *Tectonics*, *10*, 257–271.

Rosenbaum, J. M., M. Wilson, and H. Downes (1997), Multiple enrichment of the Carpathian-Pannonian mantle: Pb-Sr-Nd isotope and trace element constraints, *J. Geophys. Res.*, *102*, 14,947–14,962.

Royden, L. H. (1988), Late Cenozoic tectonics of the Pannonian Basin system, in *The Pannonian Basin: A Study in Basin Evolution*, edited by L. H. Royden and F. Horváth, *AAPG Mem.*, *45*, 27–48.

Royden, L. H., and F. Horváth (Eds.) (1988), *The Pannonian Basin: A Study in Basin Evolution*, *AAPG Mem.*, *45*, 375 pp.

Rumpler, J., and F. Horváth (1988), Some representative seismic reflection lines from the Pannonian Basin and their structural interpretation, in *The Pannonian Basin: A Study in Basin Evolution*, edited by L. H. Royden and F. Horváth, *AAPG Mem.*, *45*, 153–169.

Sandulescu, M. (1994), Overview on Romanian geology, *Rom. J. Tect. Reg. Geol*, *75*, 3–15.

Sandwell, D. T., and W. H. F. Smith (1997), Marine gravity anomalies from Geosat and ERS-1 satellite altimetry, *J. Geophys. Res.*, *102*, 10,039–10,054.

Šefara, J., M. Bielik, P. Konečný, V. Bezák, and V. Hurai (1996), The latest stage of development of the western Carpathian lithosphere and its interaction with asthenosphere, *Geol. Carpathians*, *47*, 339–347.

Seghedi, I., I. Balintoni, and A. Szakacs (1998), Interplay of tectonics and Neogene post-collisional magmatism in the intracarpathian region, *Lithos*, *45*, 483–497, doi:10.1016/S0024-4937(98)00046-2.

Seghedi, I., H. Downes, A. Szakacs, P. R. D. Mason, M. F. Thirlwall, E. Rosu, Z. Pecskay, E. Marton, and C. Panaiotu (2004), Neogene-Quaternary magmatism and geodynamics in the Carpathian-Pannonian region: A synthesis, *Lithos*, *72*, 117–146, doi:10.1016/j.lithos.2003.08.006.

Spakman, W. (1990), Tomographic images of the upper mantle below central Europe and the Mediterranean, *Terra Nova*, *2*, 542–553.

Spakman, W., S. van der Lee, and R. van der Hilst (1993), Travel-time tomography of the European-Mediterranean mantle down to 1400 km, *Phys. Earth Planet. Inter.*, *79*, 3–74.

Sperner, B., F. Lorenz, K.-P. Bonjer, S. Hettel, B. Müller, and F. Wenzel (2001), Slab break-off - abrupt cut or gradual detachment? New insights from the Vrancea Region (SE Carpathians, Romania), *Terra Nova*, *13*, 172–179.

Sperner, B., L. Ratschbacher, and M. Nemčok (2002), Interplay between subduction retreat and lateral extrusion: Tectonics of the western Carpathians, *Tectonics*, *21*(6), 1051, doi:10.1029/2001TC901028.

Sperner, B., D. Ioane, and R. J. Lillie (2004), Slab behaviour and its surface expression: New insights from gravity modelling in the SE-Carpathians, *Tectonophysics*, *382*, 51–84, doi:10.1016/j.tecto.2003.12.008.

Stulc, P. (1998), Combined effect of topography and hydrogeology on subsurface temperature—Implications for aquifer permeability and heat flow: A study from the Bohemian Cretaceous basin, *Tectonophysics*, *284*, 161–174.

Szabó, C., S. Harangi, and L. Csontos (1992), Review of Neogene and Quaternary volcanism of the Carpathian-Pannonian region, *Tectonophysics*, *208*, 243–256.

Talwani, M., J. L. Worzel, and M. Landisman (1959), Rapid gravity computations for two-dimensional bodies with application to the Mendocino submarine fracture zone, *J. Geophys. Res.*, *64*, 49–59.

Tari, G., T. Báldi, and M. Báldi-Beke (1993), Paleogene retro-arc flexural basin beneath the Neogene Pannonian Basin: A geodynamic model, *Tectonophysics*, *226*, 433–455.

Tomek, C., and J. Hall (1993), Subducted continental margin imaged in the Carpathians of Czechoslovakia, *Geology*, *21*, 535–538.

Tomek, C., and PANCARDI Colleagues (1996), PANCARDI, Dynamics of ongoing orogeny, in *EUROPROBE 1996—Lithosphere Dynamics: Origin and Evolution of Continents*, edited by D. G. Gee and H. J. Zeyen, pp. 15–23, EUROPROBE Secr., Uppsala.

Tomek, C., L. Dvořáková, I. Ibrmajer, R. Jiříček, and T. Koráb (1987), Crustal profiles of active continental collision belt: Czechoslovak deep seismic reflection profiling in the west Carpathians, *Geophys. J. R. Astron. Soc.*, *89*, 383–388.

Tomek, C., I. Ibrmajer, T. Koráb, A. Biely, L. Dvořáková, J. Lexa, and A. Zbořil (1989), Crustal structures of the west Carpathians on deep reflection seismic line 2T (in Slovak with English summary), *Mineral. Slov.*, *1/2*, 3–26.

Winkler, W., and A. Slaczka (1992), Sediment dispersal and provenance in the Silesian, Dukla and Magura flysch nappes (Outer Carpathians, Poland), *Geol. Rundsch.*, *81*, 371–382.

Wortel, M. J. R., and W. Spakman (2000), Subduction and slab detachment in the Mediterranean-Carpathian region, *Science*, *290*, 1910–1917.

Zeyen, H., and M. Bielik (2000), Study of the lithosphere structure in the western Carpathian-Pannonian basin region based on integrated modelling, *Geophys. J.*, *5*, 70–82.

Zeyen, H., J. Dérerová, and M. Bielik (2002), Determination of the continental lithosphere thermal structure in the western Carpathians: Integrated modelling of surface heat flow, gravity anomalies and topography, *Phys. Earth Planet. Inter.*, *134*, 89–104.

Zeyen, H., P. Ayarza, M. Fernàndez, and A. Rimi (2005), Lithospheric structure under the western African-European plate boundary: A transect across the Atlas Mountains and the Gulf of Cadiz, *Tectonics*, *24*, TC2001, doi:10.1029/2004TC001639.

M. Bielik, Faculty of Natural Sciences, Dept. of Applied and Environmental Geophysics, Comenius Univ., Mlynská dolina, pav. G., 842 15 Bratislava 4, Slovak Republic. (bielik@fns.uniba.sk)

J. Dérerová and K. Salman, Geophysical Institute of the Slovak Academy of Sciences, Dúbravská cesta 9, 842 28 Bratislava, Slovak Republic. (geofjade@savba.sk)

H. Zeyen, Département des Sciences de la Terre, UMR 8146, Univ. é de Paris-Sud, IDES Bât. 504, F-91504 Orsay Cedex, France. (zeyen@geol.u-psud.fr)